Jurnal
Teknologi

Full Paper

FEASIBILITY STUDY OF USING TELESCOPIC INVERTED PENDULUM MODEL TO REPRESENT A THREE LINK SYSTEM FOR SIT TO STAND MOTION

Muhammad Fahmi Miskon*, Mohd Zaki Ghazali, Mohd Bazli Bahar, Chew Xiao Lin, Fariz Ali

Universiti Teknikal Malaysia Melaka, Malaysia
Center of Excellence in Robotics and Industrial Automation

Article history
Received
15 May 2015
Received in revised form
1 July 2015
Accepted
11 August 2015

*Corresponding author
fahmimiskon@utem.edu.my

Graphical abstract

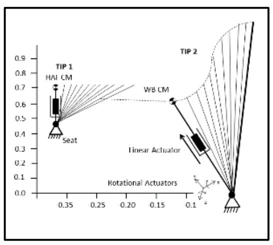

Abstract

Sit to stand (STS) is a very challenging motion for any humanoid robotic system. In humanoid robotics field, the STS motion on the sagittal plane can be predicted using three-link robot inverse kinematic and dynamic model. However, a three-link model is complicated and requires high computational resource to compute. Hence, in this paper a much simpler model namely telescopic inverted pendulum is proposed. The objective of this project is to model and validate sit to stand motion of humanoid robot using telescopic inverted pendulum model. In order to validate the model, simulated joint torques using both three-link and TIPS model are compared using MATLAB software. Result shows that there is a linear relationship between Telescopic Inverted Pendulum with the 3 Link model thus, it is feasible to use TIPS to represent STS motion of a three-link multi-segment robot.

Keywords: Telescopic Inverted Pendulum, Sit to Stand, three-link model

1.0 INTRODUCTION

The study of sit to stand motion (STS) gives high impact to the robotics field particularly in the field of rehabilitation [1], exoskeleton [2] as well as humanoid robotics[3][4]. In humanoid robotics field, the STS study has not been given emphasis until recently [5].

A proper trajectory planning will ensure stable STS motion. Until now, researchers in the humanoid robotics field that investigates STS use trajectory acquired from direct observation of human STS. Some determine the trajectory heuristically. These approaches take time and the behavior of the system cannot be predicted. STS in varying environment is also difficult to be implemented. For these reasons dynamic model of STS motion is needed.

In the field of humanoid robotics, recorded human STS motion is directly translated into humanoid robot STS trajectory [5]–[7]. Alternatively, STS trajectory is determined heuristically [8]. No STS motion model is developed or used to plan the appropriate trajectory for a designated humanoid robot. In the field of biomechanics, several model of STS motion has been developed including the three link (3L) inverted pendulum [9] [10], two-link elastic inverted pendulum [11] as well as single rigid pendulum [12] and telescopic single pendulum (TIP) [13] to study the structural stability, balance and energy transfer during STS task. Of all the models, TIP model is more suitable for planning and analyzing humanoid robot STS motion trajectory since it directly represents the whole body motion or the COM of the robot in Cartesian space [14][15]. TIP model also is much simpler when compared to 3L model that is commonly used.

However, the suitability of TIP model to represent STS motion of humanoid robot is unknown and has not been validated yet. Also, the resulting ground reaction force (N) from motion generated by the TIP model has not been investigated thus the stability of the robot when applying the STS trajectory from the model is unknown.

For this reasons, this paper presents a study conducted to see the feasibility of using TIP to model STS motion of humanoid robot.

2.0 BACKGROUND OF STS MOTION

Previous studies represent STS motions having several phases. Some studies proposed that STS consists of two phases i.e. initial forward trunk lean and upward extension. Others proposed STS to have three phases consisting of initial phase, seat unloading and ascending phase [16], [17]. This project is based on the latter which detail is shown in Figure 1.

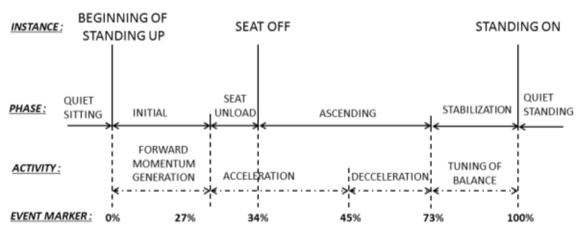

Figure 1 Stand up cycle diagram, displaying phase, activity, event marker and instance

According to [18], during the initial phase, Head Arm Torso (HAT) leans forward up to 27% of the complete cycle. During this period, the momentum built allows the HAT to unload and accelerate towards seat off instance at 34% of the complete cycle. At this instance, the STS cycle starts entering the ascending phase. During this period the whole body (WB) ascends to standing position. Upon reaching 45% of the complete cycle, WB slowly decelerates until the STS cycle reaches 73%. Then the WB stabilizes towards the end of STS motion. Finally, when the cycle reaches 100%, the WB is in total standing up position.

In TIP model, the phases are realized as TIP1 for representing initial phase (Phase 1), and TIP 2 for representing ascending phase (Phase 3) as shown in Figure 2. Between this TIP 1 and TIP 2 is unloading phase (Phase 2) which is not explicitly represented by any model in this paper.

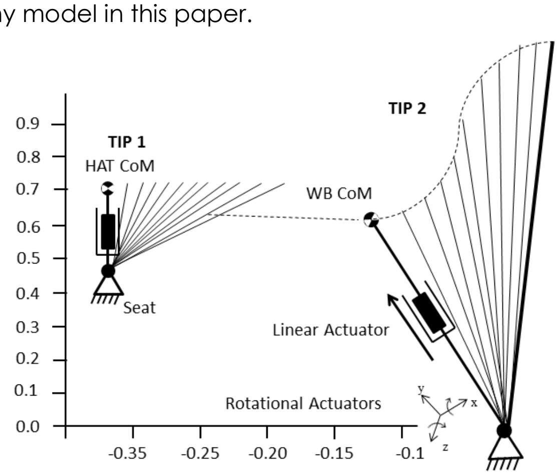

Figure 2 Schematic presentation of TIP model

Referring to Figure 2, only one segment moves forward during TIP 1 which is the HAT CoM. The CoM is set to move in a straight line, mimicking the result of trunk muscle movement when leaning forward [19]. Towards the end of TIP 1, the momentum build made the HAT lift off before TIP 2 is used to represent the movement of WB CoM during ascending.

TIP and 3L models during Phase 1 and Phase 3 are illustrated in Figure 3 and 4. Both foots are fixed to the floor and assumed to be parallel to each other. In Phase 1, only Link 3 moves in the three-link model hence TIP1 is comparable to only Link 3. Both links move in the clockwise direction.

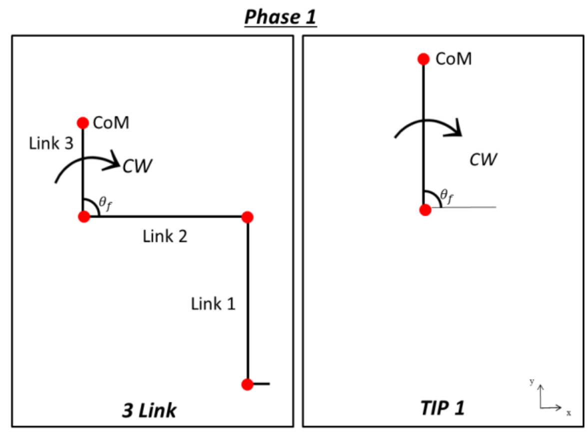

Figure 3 Comparison movement of the 3L and TIP during the Phase 1

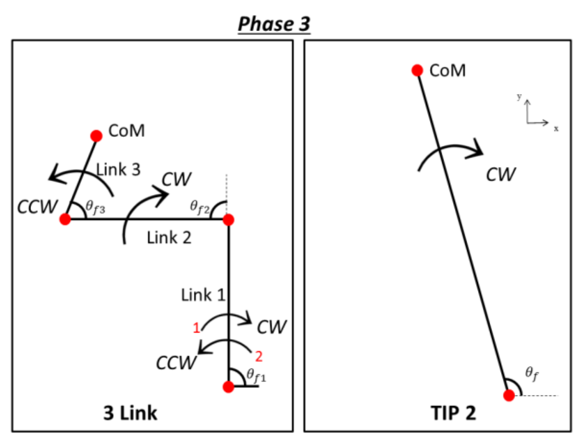

Figure 4 Comparison movement of the 3L and TIP during the Phase 3

In Phase 3, all links in the 3L models move hence TIP2 is comparable to all the three links. The first link of the 3L model is set to be the lower legs, second link to be the thighs and third link represents the upper body, including arms and head. As for TIP2 model, the three links is simplified to be represented with one extendable link. Link 1 of the 3L model moves in CW direction before going CCW during ascending. As for link 2, the momentum from the motion in phase 1 will lift it upwards in CW movement. Lastly for link 3, from moving forward in phase 1, it will counter back to move in CCW direction as it approaching the final standing position in STS motion.

3.0 SIMULATION

For the purpose of validation, a 3L multi-segment robot and TIPS are simulated in MATLAB software to compare the kinematics and dynamics behavior of both models during STS motion. As depicted in Figure 2, for the TIPS model, the STS trajectory of the end-effector in Cartesian space in both Phase 1 and Phase 3 is represented using linear (Phase 1) and cubic polynomial equation (Phase 3). To ensure similarity, 3L robot end-effector's trajectory in Cartesian space is also set according to the same linear and cubic polynomial equations. Then the rotations angles and angular velocity of the hip, knee and ankle joint of the 3L model is obtained using inverse kinematic and Jacobians theorem [20].

The linear equation used in Phase 1 has an initial value of y = 0.62m and x = -0.393m, and the final position of y = 0.62m and x = -0.25m while the position interval is 0.00135m. The linear equation is represented by Equation 1.

$$y(x) = a_0 + a_1 x \qquad (1)$$

Then, by assuming the initial position for Phase 3 is y=0.62m and x = -0.2m, the final COM position is y=1.022 m and the position interval is 0.02m, the COM trajectory equation for TIP 2 is as equation 2:

$$y(x) = b_0 + b_1 x + b_2 x^2 + b_3 x^3 \qquad (2)$$

Where x and y represents the COM position in Cartesian space.

3.1 Telescopic Inverted Pendulum Model

TIP output torque [13] is represented by the following equations.

$$F = m a_{com}.\hat{l} - mg.\hat{l} \qquad (3)$$

$$C = \frac{d([J]\omega)}{dt} + \omega \times [J]\omega - \hat{l} \times mg \qquad (4)$$

$$[J] = \begin{bmatrix} ml^2 & 0 & 0 \\ 0 & 0 & 0 \\ 0 & 0 & ml^2 \end{bmatrix} \qquad (5)$$

$$\omega = \begin{bmatrix} 0 & 1 & 0 \\ \sin\theta_f & 0 & 1 \\ \cos\theta_f & 0 & 0 \end{bmatrix} \begin{bmatrix} \dot{\theta}_s \\ \dot{\theta}_f \\ 0 \end{bmatrix} \qquad (6)$$

where F and C is the force and couple vectors supplied by the model's actuator, m is the mass, $\hat{l}$ indicates the link versor, g is the gravity, J is the inertia matrix, ω is the angular velocity, a_{com} is the acceleration of center of mass, $\dot{\theta}_f$ and $\dot{\theta}_s$ (see Figure 3 and 4) angular velocity on the joints. The dynamic parameter for TIP model simulation is as Table 1. The values are based on the average of adult mass as presented in [21] .

Table 1 Dynamic parameter of TIP model simulation

Phase	Mass (Kg)	Length (m)
Phase 1	45.990	0.294
Phase 3	70.372	1.022

3.2 Three-link Multi Segment Model

Since Phase 1 only involved the movement of upper body, therefore only the torque of 3L model for hip joint 3 involved. The torque is calculated based on [21] as represented in Equation 7:

$$\tau_3 = M_{33}\ddot{\theta}_3 + D_3\dot{\theta}_3 + g_3 \qquad (7)$$

where τ_3 is the torque for τ_{3l_phase1}. Phase 3 involves the whole body movement thus torque at all joints are involved as shown in Equation 8.

$$\begin{bmatrix} \tau_1 \\ \tau_2 \\ \tau_3 \end{bmatrix} = \begin{bmatrix} M_{11} & M_{12} & M_{13} \\ M_{21} & M_{22} & M_{23} \\ M_{31} & M_{32} & M_{33} \end{bmatrix} \begin{bmatrix} \ddot{\theta}_1 \\ \ddot{\theta}_2 \\ \ddot{\theta}_3 \end{bmatrix} + \begin{bmatrix} h_1 \\ h_2 \\ h_3 \end{bmatrix} + \begin{bmatrix} g_1 \\ g_2 \\ g_3 \end{bmatrix} + \begin{bmatrix} D_1 & 0 & 0 \\ 0 & D_2 & 0 \\ 0 & 0 & D_3 \end{bmatrix} \begin{bmatrix} \dot{\theta}_1 \\ \dot{\theta}_2 \\ \dot{\theta}_3 \end{bmatrix} \qquad (8)$$

$$= \mathrm{M}\ddot{\boldsymbol{\theta}} + \mathrm{h} + \mathrm{g} + \mathrm{D}\,\dot{\boldsymbol{\theta}}$$

where, $\boldsymbol{\theta}$ is the joint angle, $\dot{\boldsymbol{\theta}}$ is the joint angular velocity and $\ddot{\boldsymbol{\theta}}$ denote the joint angular of the i^{th} joint as indicate in Equation 6 and 7. The matrix $\mathbf{M}$ = [$\mathbf{M}\, ij$] (i =1~3, j =1~3) and the vectors $\boldsymbol{h}$ = $[h1, h2, h3]^T$ $\boldsymbol{g}$ = $[g1, g2, g3]^T$] and $\boldsymbol{D}\dot{\boldsymbol{\theta}}$ represent the inertia matrix, the Coriolis and centrifugal force vector,the gravity force vector, and the viscous force vector respectively and superscript $\boldsymbol{T}$ denotes the transpose of a vector.

Table 2 Dynamic parameter of 3L model simulation

Parameter	Link 1	Link 2	Link 3
L_i (m)	0.335	0.393	0.736
Lc_i (m)	0.191	0.224	0.294
m_i (kg)	7.738	16.644	45.99
I_i (kg)	0.988	2.572	41.476
D_i (Nm.s/rad)	0.440	1.050	3.750

Table 2 summarizes the dynamic parameter for the model simulation where $\boldsymbol{m_i}$ represents the mass of the i-th link, L_i, Lc_i, and I_i are the length of the i-th link, distance from the i-th joint to the center of mass of the i-th link, and the moment of inertia around the center of mass of the i-th link, respectively. As for D_i is the coefficient of viscosity of the i-th joint; **g** is the acceleration of gravity (= $9.8\text{m}/\text{sec}^2$). The values of m_i, Lc_i, and L_i were estimated from the measured link lengths L_i and the body weight m_i referring to references [22].

4.0 RESULTS AND DISCUSSION

As shown in Figure 5, during phase 1, both 3L joint torque τ_{3l_phase1} and TIP 1 torque $\tau_{TIP1\_\text{phase1}}$ have similar pattern. For both models, the pattern is linear indicating torques are decreasing as the HAT goes to clockwise (CW) direction. Only link 3 for 3L model and hip for TIP 1 is moving forward to simulate the movement of HAT.

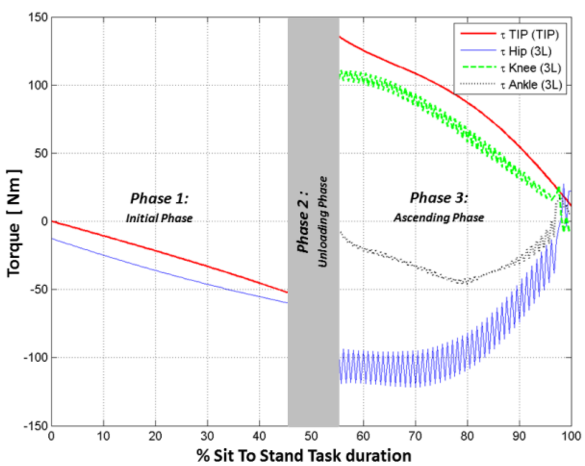

Figure 5 Relationship of TIP Model and 3L model

Towards the end of phase 1, $\tau_{TIP1\_\text{phase1}}$ stops at **-54.55 Nm** while τ_{3l_phase1} stops at **-61.24 Nm**. Negative value indicates the movement into negative region and it was projected as decreasing while actually it is increasing. Thus, its explain the momentum from initial state towards the end of phase 1. Higher torque at the end of the phase 1 is to counter the force by inertia moment.

As mentioned in [13], there is an unloading phase as soon phase 1 ended. During this phase, HAT is flexing while decelerating. As its flexion ceases, the hip joint is momentarily blocked and it allows the momentum transfer from the HAT to the WB through rotations about the knee and/or ankle joints [13] . The duration of this phase took about 10% from total STS cycle [13].

Phase 3 in Figure 5 shows the pattern of both 3L and TIP model. The result shows that the pattern curved to zero value towards the end of Phase 3. The reason is because all the links is decelerating as the STS motion approaching full standing position.

Slightly after unloading phase, the momentum from Phase 1 made the $\tau_{TIP2\_\text{phase3}}$ start at **142.61 Nm** and slowly decreases to **11.44 Nm** towards the end of phase 3. As for 3L model, the value of $\tau_{3l\_ankle\_phase3}$ starts with **21.42 Nm** as it decreases to 77% before it increases to **5.73 Nm**. The plausible reason behind this is Link 1 is moving in CW direction first before it moves back in CCW direction to counter the inertia from phase 1 STS cycle. When all links is moving to stand up, Link 1 moves back CCW to give a result of standing straight.

Meanwhile, $\tau_{3l\_knee\_phase3}$ starts with **111.60 Nm** from the momentum in Phase 1 and has pattern similar with $\tau_{TIP2\_\text{phase3}}$. It is interesting to see that as the $\tau_{TIP2\_\text{phase3}}$ decreases the same thing happened to the $\tau_{3l\_knee\_phase3}$.

On the other hand, $\tau_{3l\_hip\_phase3}$ shows a decreasing pattern from **-122.94 Nm** maintaining the trajectory until 70% of STS cycle before it is increasing rapidly for the last 30% of the cycle. This may be due to the momentarily block of hip joint during standing up. When it reaches 70% duration, all joint moves simultaneously to enable the WB to stand up, thus make the $\tau_{3l\_hip\_phase3}$ increases.

Based on the observation of the result in Figure 5, both τ_{3l_phase1} and $\tau_{TIP1\_phase1\_}$ are analyzed using Root Mean Square Error (RMSE). RMSE gives an insight on the difference between two values that change over time. Small RMSE between the two values indicates that both values are similar. The result acquired is **12.81Nm.** The value is considered small when compared to the range of torque involve during the whole STS motion. From this we can say that both TIP and 3L models represents Phase 1 of STS motion similarly with each other.

The relationship between τ_{3l_phase1} and $\tau_{TIP1\_phase1\_}$ is then further investigated by plotting both data versus each other as shown in Figure 6. Curve fitting is then implemented on the plotted data by using 1st degree polynomial equation. The goodness of fit indicates that R-square is equal to **0.9913**. Noted that the closer R-square is to 1, the better the plotted data fit a straight line. With the value of **0.9913**, the data it almost on a straight line thus, strengthening the fact that the relationship between these two model is linear.

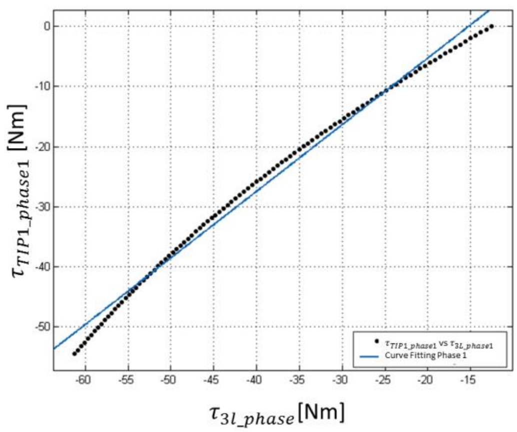

Figure 6 Curve fitting of $\tau_{TIP1\_\text{phase1}}$ vs τ_{3l_phase1} data using 1st degree polynomial equation

The result of RMSE values for Phase 3 is shown in Table 3. The lowest RMSE value belongs to torque at knee joint, $\tau_{3l\_knee\_phase3}$ which is **20.94 Nm**. This shows that $\tau_{3l\_knee\_phase3}$ is highly similar to $\tau_{TIP2\_\text{phase3}}$.

Table 3 RMSE value for phase 3

Link/Joint	RMSE Value
Link 1/Ankle	117.88
Link 2/Knee	20.94
Link 3/Hip	185.05

The relationships between $\tau_{3l\_ankle\_phase3}$ and $\tau_{TIP2\_\text{phase3}}$, between $\tau_{3l\_knee\_phase3}$ and $\tau_{TIP2\_\text{phase3}}$ and between $\tau_{3l\_hip\_phase3}$ and $\tau_{TIP2\_\text{phase3}}$ are further investigated by plotting them versus each other. Figure 7 shows the results of the plot. From the figure we can see how $\tau_{3l\_knee\_phase3}$ and $\tau_{3l\_hip\_phase3}$ could potentially have linear relationship with $\tau_{TIP2\_\text{phase3}}$. However, $\tau_{3l\_ankle\_phase3}$ obviously does not fit to $\tau_{TIP2\_\text{phase3}}$.

Curve fitting is implemented on the plotted data by using 1st degree polynomial equation. Figure 8 to 10 show the results of the curve fitting. The goodness of fit analysis using R square is tabulated in Table 4. As expected, the plotted data with $\tau_{3l\_knee\_phase3}$ fit most to a straight line with R square value of 0.9685 followed by $\tau_{3l\_hip\_phase3}$ with R square value of 0.7525. This indicates that $\tau_{3l\_knee\_phase3}$ has a strong linear relationship with $\tau_{TIP2\_\text{phase3}}$. On the other hand, plotted data with $\tau_{3l\_ankle\_phase3}$ only has R square of 0.02893 hence support that there is no linear relation between $\tau_{3l\_ankle\_phase3}$ and $\tau_{TIP2\_\text{phase3}}$.

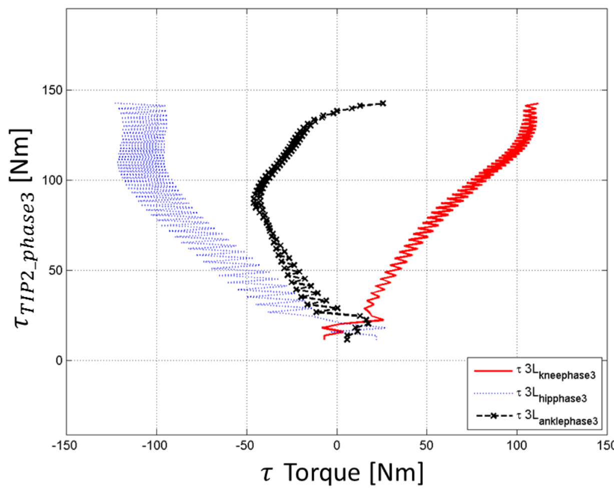

Figure 7 Relationship of $\tau_{TIP2\_\text{phase3}}$ vs τ_{3l_phase3}

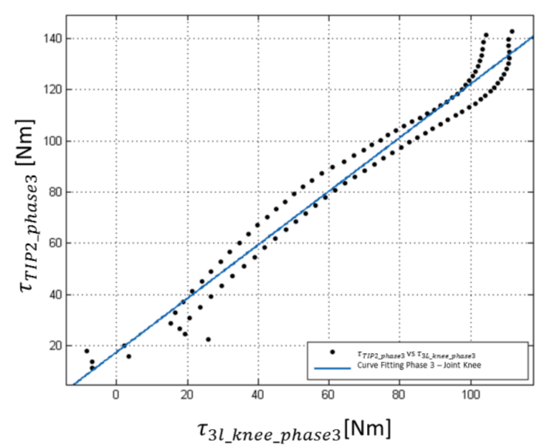

Figure 8 Curve Fitting of $\tau_{TIP2\_\text{phase3}}$ vs $\tau_{3l\_knee\_phase3}$ data using 1st degree polynomial equation

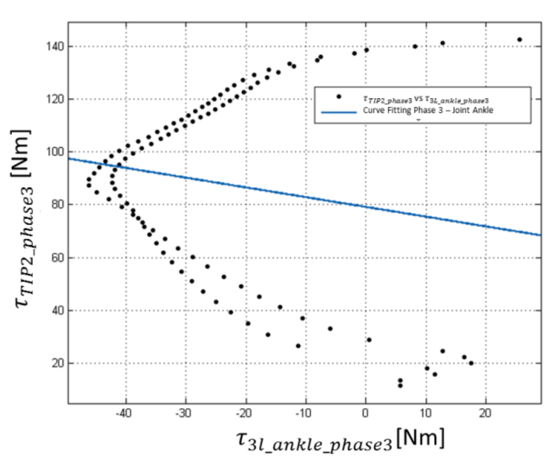

Figure 9 Curve fitting of $\tau_{TIP2\_\text{phase3}}$ vs $\tau_{3l\_ankle\_phase3}$

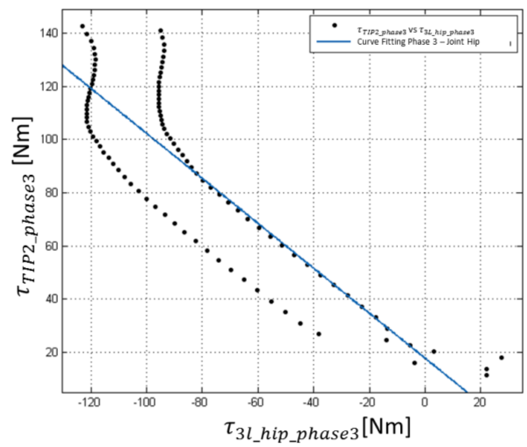

Figure 10 Curve fitting of $\tau_{TIP2\_\text{phase3}}$ VS $\tau_{3l\_hip\_phase3}$ data using 1st degree polynomial equation

Table 4 Result R-square of Curve Fitting

Curve Fitting	R-square
$\tau_{TIP2\_\text{phase3}}$ VS $\tau_{3l\_ankle\_phase3}$	0.02893
$\tau_{TIP2\_\text{phase3}}$ VS $\tau_{3l\_knee\_phase3}$	0.9685
$\tau_{TIP2\_\text{phase3}}$ VS $\tau_{3l\_hip\_phase3}$	0.7525

Another analysis performed on the simulated data is Analysis of Variance Type 1 (ANOVA1). ANOVA1 performs a balanced one-way comparison with the means of two or more sets of data, where each set represents an independent sample containing mutually independent observations. ANOVA1 returns p-value under the null hypothesis that all samples in X are drawn from populations with the same mean. The hypothesis H_0 is to reject any relationship between TIP model and 3L muti-segment model, while H_1 is to accept the relationship between both TIP and 3L model. The result for phase 1 gives **p = 3.21**$\times$ $\mathbf{10^{-16}}$ and **f=5.54**. Since p<f, there is a relationship between TIP and 3L model in Phase 1. As for Phase 3, the results are shown as Table 4 below.

Table 4 Result of ANOVA1 test between the torque of TIP and 3L model in Phase 3

Test	P	F	P>F
Link 1	1	0.09	True
Link 2	1.02 $\times$ 10^{-16}	10.39	False
Link 3	1	0.01	True

From the result in Table 4, we can see both Link 1 and Link 3 giving **p>f is true,** meaning H_0 was accepted. So, there is no relationship between both $\tau_{3l\_ankle\_phase3}$ and $\tau_{3l\_hip\_phase3}$ with $\tau_{TIP2\_\text{phase3}}$. But for link 2, **p<f,** hence the H_0 hypothesis is false and rejected. From this we can say there is a relationship between $\tau_{TIP2\_\text{phase3}}$ and $\tau_{3l\_knee\_phase3}$.

In overall, during Phase 1, the analysis results show hip joint torque is similar and has linear relationship with TIP1 joint torque. In Phase 3, it is interesting to see that the evidence from all analysis made indicates that knee torque is most similar and has almost linear relationship with TIP2 torque when compared to hip and ankle torque. This is due to the fact that in STS motion knee joint is the main pivoting point during ascending hence similar to the function of rotating axis of θ_f in TIP2.

5.0 CONCLUSION

Simulation work has been conducted to determine whether it is feasible to represent a three-link system by using a Telescopic Inverted Pendulum model particularly for representing STS motion. TIP model and 3L model were compared during Phase 1 and Phase 3 of STS motion.

The result shows that the RMSE between τ_{3l_phase1} and $\tau_{TIP1\_phase1\_}$ and RMSE between $\tau_{TIP2\_\text{phase3}}$ and $\tau_{3l\_knee\_phase3}$ are very low, relative to the range of torque involve and relative to the torque of other joints with value of **12.81Nm** (Phase 1, between hip torque and TIP1) and **20.94Nm** (Phase 3, between knee torque and TIP2). In both cases, the R-square value from curve fitting to a 1st degree polynomial model is also very good with value of **0.9913** (Phase 1, between hip torque and TIP1) and **0.9685** (Phase 3, between knee torque and TIP2). Finally the result of the ANOVA1 test shows that both have **p<f** (for both (Phase 1, between hip torque and TIP1) and (Phase 3, between knee torque and TIP2)). However, RMSE, Regression and ANOVA1 test in Phase 3 between $\tau_{3l\_hip\_phase3}$ and $\tau_{TIP2\_\text{phase3}}$ and between $\tau_{3l\_ankle\_phase3}$ and $\tau_{TIP2\_\text{phase3}}$ show negative results. No direct relationship is found between TIP and 3L model for ankle and hip joints.

In conclusion, it is feasible to use Telescopic Inverted Pendulum (TIP) to model the torque of 3L multi segment robot particularly for Link 3 (hip joint) during Phase 1 and for Link 2 (knee joint) during Phase 3. However, further studies need to be carried be carried out to strengthen the theory by performing physical experiments and testing the theory from various angles including the effect of changing lengths and masses as well as determining how hip and ankle joint could be included in the model.

Acknowledgement

The authors would like to thank the Ministry of Education Malaysia for funding this project under the Fundamental Research Grant Scheme and for the moral and technical support from the Universiti Teknikal Malaysia Melaka (UTeM) especially from the Robotics and Industrial Automation (RIA) research group in the Centre of Excellence in Robotics and Industrial Automation (CeRIA). Order of authorship

was determined by the amount of overall contribution towards making the project successful.

Nomenclature

STS	Sit to stand	F	Force
CoM	Centre of Mass	C	Couple Vetor
HAT	Head Arm Torso	τ	Tau. Torque
WB	Whole Body	τ_{3l_phase1}	Torque of three link during phase 1
TIP	Telescopic Inverted Pendulum	τ_{3l_phase3}	Torque hip of three link during phase 3
TIP 1	TIP model representing HAT movement only	τ_{TIP1_phase1}	Torque of TIP 1 during phase 1
TIP 2	TIP model representing WB movement only	τ_{TIP2_phase3}	Torque of TIP 2 during phase 3
3L	Three-link	$\tau_{3l\_knee\_phase3}$	Torque knee of three link during phase 3
g	gravity	$\tau_{3l\_ankle\_phase3}$	Torque ankle of three link during phase 3
J	Inertia matrix	$\tau_{3l\_hip\_phase3}$	Torque hip of three link during phase 3
l	Link versor	CW	Clockwise
CCW	Counter Clockwise		

References

[1] O. C. Jr., Y. Hirata, Z. Wang, and K. Kosuge. 2006. Approach in Assisting a Sit-to-Stand Movement Using Robotic Walking Support System, *2006 IEEE/RSJ Int. Conf. Intell. Robot. Syst*. 4343-4348.

[2] K. a. Strausser and H. Kazerooni. 2011. The Development And Testing Of A Human Machine Interface For A Mobile Medical Exoskeleton. *2011 IEEE/RSJ Int. Conf. Intell. Robot. Syst*. 4911-4916.

[3] F. Ali, A. Z. H. Shukor, M. F. Miskon, M. K. M. Nor, and S. I. M. Salim. 2013. 3-D Biped Robot Walking Along Slope With Dual Length Linear Inverted Pendulum Method (DLLIPM). *Int. J. Adv. Robot. Syst*. 10.

[4] N. L. a Shaari, M. Razmi, B. Razali, M. F. Miskon, and I. S. Isa, 2013. Parameter Study of Stable Walking Gaits for Nao Humanoid Robot. 16-23.

[5] M. Mistry, A. Murai, K. Yamane, and J. Hodgins, Dec. 2010. Sit-to-stand Task On A Humanoid Robot From Human Demonstration. *2010 10th IEEE-RAS Int. Conf. Humanoid Robot*. 2: 218–223.

[6] S. Pchelkin, A. Shiriaev, L. Freidovich, U. Mettin, S. Gusev, and W. Kwon, Dec. 2010. Natural Sit-Down And Chair-Rise Motions For A Humanoid Robot. *49th IEEE Conf. Decis. Control*. 1136-1141.

[7] M. Sadeghi, M. Emadi Andani, M. Parnianpour, and A. Fattah. 2013. A Bio-Inspired Modular Hierarchical Structure To Plan The Sit-To-Stand Transfer Under Varying Environmental Conditions. *Neurocomputing*. 118: 311-321.

[8] K. Qi. 2009. Analysis of the State Transition for a Humanoid Robot SJTU-HRI from Sitting to Standing. 1922–1927.

[9] H. Hemami and V. C. Jaswa. 1978. On a Three-Link Model of the Dynamics of Standing up and Sitting down *IEEE Trans. Syst. Man. Cybern.* 8(2): 115-120.

[10] J. M. Ć, R. Kamnik, V. Zanchi, and M. Munih. 2007. Model Based Inertial Sensing for Measuring the Kinematics of Sit-to-Stand Motion. 8-13.

[11] R. Aissaoui, R. Ganea, and K. Aminian, Apr. 2011, Conjugate Momentum Estimate Using Non-Linear Dynamic Model Of The Sit-To-Stand Correlates Well With Accelerometric Surface Data. *J. Biomech.* 44(6): 1073-7.

[12] Y. Pai and J. Patton. 1997. Center Of Mass Velocity. 30(4): 1-7.

[13] E. Papa and A. Cappozzo. 1999. A Telescopic Inverted-Pendulum Model Of The Musculo-Skeletal System And Its Use For The Analysis Of The Sit-To-Stand Motor Task. *J. Biomech.* 32(11): 1205-12.

[14] B. Bahar, M. F. Miskon, N. A. Bakar, A. Z. Shukor, and F. Ali. 2014. *Australian Journal of Basic and Applied Sciences*. 8(February): 168-182.

[15] H. Robotics. 2014. STS Motion Control using NAO Humanoid Robot. 8(2): 95-108.

[16] P. O. Riley, M. L. Schenkman, R. W. Mann, and W. A. Hodge. 1991. Mechanics of a Constrained Chair-Rise. *J. Biomech.* 24(1): 77-85.

[17] P. J. Millington, B. M. Myklebust, and G. M. Shambes. 1992. Biomechanical Analysis Of The Sit-To-Stand Motion In Elderly Persons. *Arch. Phys. Med. Rehabil.* 73: 609-617.

[18] A. Kralj, R. J. Jaeger, and M. Munih. 1990. Analysis Of Standing Up And Sitting Down In Humans: Definitions And Normative Data Presentation. *J. Biomech*. 23: 1123-1138.

[19] E. Papa and A. Cappozzo. 2000. Sit-to-stand Motor Strategies Investigated In Able-Bodied Young And Elderly Subjects *J. Biomech.* 33(9): 1113-1122.

[20] J. J. Craig. 2005. *Introduction-to-ROBOTICS-craig.pdf*. Pearson Education Inc.

[21] K. Wada and T. Matsui. 2013. Optimal Control Model for Reproducing Human Sitting Movements on a Chair and its Effectiveness. *J. Biomech. Sci. Eng.* 8(2): 164-179.

[22] D. a Winter. 1990. *Biomechanics and Motor Control of Human Movement*.